A Proteomic Investigation of Drug-Induced Steatosis in Rat Liver

ARTICLE *in* CHEMICAL RESEARCH IN TOXICOLOGY · JUNE 2004

Impact Factor: 3.53 · DOI: 10.1021/tx034203n · Source: PubMed

11 AUTHORS, INCLUDING:

Paul C Guest
University of Cambridge
167 PUBLICATIONS **2,711** CITATIONS
SEE PROFILE

Russell Mortishire-Smith
Waters Corporation
61 PUBLICATIONS **2,304** CITATIONS
SEE PROFILE

A Proteomic Investigation of Drug-Induced Steatosis in Rat Liver

Georgina Meneses-Lorente,*[,†,‡] Paul C. Guest,[†,‡] Jeffrey Lawrence,[§] Nagaraja Muniappa,[§] Michael R. Knowles,[†] Heather A. Skynner,[†] Kamran Salim,[†] Ileana Cristea,[∥] Russell Mortishire-Smith,[†] Simon J. Gaskell,[⊥] and Alan Watt[†]

Merck Sharp & Dohme Neuroscience Research Centre, Terlings Park, Harlow, Essex, CM20 2QR, United Kingdom, Department of Safety Assessment, Merck Research Laboratories, West Point, Pennsylvania 19486, Laboratory of Mass Spectrometry and Gaseous Ion Chemistry, The Rockefeller University, New York 10021, and The Michael Barber Center for Mass Spectrometry, UMIST, Manchester M60 1QD, United Kingdom

Received October 3, 2003

A significant problem faced by pharmaceutical companies today is the failure of lead compounds in the later stages of development due to unexpected toxicities. We have used two-dimensional differential in-gel electrophoresis and mass spectrometry to identify a proteomic signature associated with hepatocellular steatosis in rats after dosing with a compound in preclinical development. Liver toxicity was monitored over a 5 day dosing regime using blood biochemical parameter measurements and histopathological analysis. As early as 6 h postdosing, livers showed hepatocellular vacuolation, which increased in extent and severity over the course of the study. Alterations in plasma glucose, alanine aminotransferase, and aspartate aminotransferase were not detected until the third day of dosing and changed in magnitude up to the final day. The proteomic changes were observed at the earliest time point, and many of these could be associated with known toxicological mechanisms involved in liver steatosis. This included up-regulation of pyruvate dehydrogenase, phenylalanine hydroxylase, and 2-oxoisovalerate dehydrogenase, which are involved in acetyl-CoA production, and down-regulation of sulfite oxidase, which could play a role in triglyceride accumulation. In addition, down-regulation of the chaperone-like protein, glucose-regulated protein 78, was consistent with the decreased expression of the secretory proteins serum paraoxonase, serum albumin, and peroxiredoxin IV. The correlation of these protein changes with the clinical and histological data and their occurrence before the onset of the biochemical changes suggest that they could serve as predictive biomarkers of compounds with a propensity to induce liver steatosis.

Introduction

Toxicological studies require a considerable amount of resources during the development of new pharmaceuticals. Approximately 30% of new compounds fail due to toxicity, resulting in increased costs and delays in successful drug development (*1*). Toxicity often does not become apparent until the preclinical or clinical development stages of drug discovery when compound testing is initiated in animal models or humans. Therefore, the ability to achieve prediction of toxicity within an in vivo/in vitro setting would represent a big step forward in accelerating any drug discovery program.

Proteomics is a system approach for the global study of protein expression changes (*2*). This technology can provide information on gene function, disease processes, and mechanisms of drug action at several stages in the drug discovery pipeline and pave the way for improved and speedier drug discovery strategies to be implemented. Proteomics profiling used in combination with histological and clinical chemistry studies is likely to help to delineate the mechanisms involved in drug toxicity or yield protein signatures associated with certain classes of toxicities.

In house in vivo safety studies in mice, rats, and monkeys identified a compound [designated compound A (**1**)] that was hepatotoxic causing hepatocellular vacuolation or steatosis, centrilobular granular hypertrophy, single cell necrosis, and periductal inflammation (*3*). While the mechanisms underlying these toxic events are unknown, previous in vitro and metabonomics work showed that compound A disrupted the β-oxidation pathway (*3*). Drug-induced steatosis is a serious issue within the pharmaceutical industry as extensive microvesicular steatosis may lead to liver failure (*4*). Previous reports have shown 4,4′-diethylaminoethoxyhexestrol, amiodarone, and perhexiline, which are known to cause steatohepatitis in humans, inhibit both β-oxidation and respiration pathways in rat hepatocytes (*5*−*8*).

In the present study, we have used fluorescence two-dimensional (2D) differential in-gel electrophoresis (DIGE) to investigate the mechanism of compound A-induced toxicity in rats after 6 h of treatment. We show that the proteomics data obtained for compound A-induced toxic-

* To whom correspondence should be addressed. Tel: (0)1279-440169. Fax: (0)1279-440390. E-mail:georgina_meneseslorente@merck.com.
† Merck Sharp & Dohme Neuroscience Research Centre.
‡ Authors contributed equally to the generation of the manuscript.
§ Merck Research Laboratories.
∥ The Rockefeller University.
⊥ UMIST.

10.1021/tx034203n CCC: $27.50
Published on Web 04/13/2004

ity correlate with the clinical and histological data and most importantly that the potential mechanistic-induced toxicity-related proteins are changed before biochemical parameters are affected.

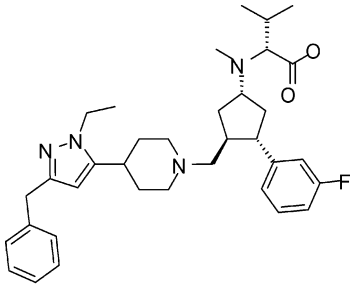

1

Materials and Methods

Animals. Female rats [Crl:CD (SD)IGS BR; ca. 6 weeks of age] were obtained from Charles River. All animal husbandry procedures were in accordance with the Guide for the Care and Use of Laboratory Animals (NIH Publication, Vol. 25, No. 28, August 16, 1996; http://grants1.nih.gov/grants/guide/notice-files/not96-208.html), and all experimental procedures were approved by Institutional Animal Care and Use Committees (IACUC) of the facilities in which the studies were conducted. All animals were housed in standard laboratory animal facilities and were provided free access to water and, except during urine collection, measured amounts of food.

Rats received 16 g/day of PMI Certified Rodent Diet, and water was available ad libitum. Food was withdrawn overnight prior to scheduled blood collections for serum biochemical determinations and prior to scheduled necropsies. Treatments were administered by oral gavage once daily for up to 5 days. Groups of 18 rats received either 250 mg/kg/day compound A, 500 mg/kg/day compound A, or vehicle [0.5% (w/v) methylcellulose in deionized water]. The treatment groups were divided further into six groups of three animals each. Serum biochemical examinations [glucose, alanine aminotransferase (ALT), and aspartate aminotransferase (AST)] (*9*) were conducted on all animals prior to necropsy. Animals were exsanguinated, and livers were removed for protein extraction and histopathological examination.

Histology. Livers from vehicle- and compound A-treated animals were fixed in 10% neutral buffered formalin (NBF) and processed according to standard laboratory procedures. Five micrometer thick paraffin-embedded sections were stained with hematoxylin and eosin and examined microscopically. In addition, cryosections of NBF fixed livers were stained for neutral lipids using Oil Red O stain and examined microscopically.

Protein Extraction. Livers were homogenized separately using a Polytron homogenizer (Kinematica, Switzerland) in 2 mL of buffer 1 [30 mM Tris (pH 8) containing 8 M urea] and centrifuged at 100 000*g* for 30 min at 4°C in a TL30 rotor (Beckman, Palo Alto, CA). The supernatants were removed and stored at −80 °C until further analysis. The pellets were homogenized in 2 mL of buffer 2 [30 mM Tris (pH 8) containing 7 M urea, 2 M thiourea, and 4% CHAPS], and the centrifugation was repeated. The final supernatants were retained and stored at −80 °C until further analysis. Equal aliquots from all individual liver extracts were also used to generate a standard pool.

Protein−Cyanine Dye Labeling. Individual and pooled aliquots of liver homogenates were labeled covalently with cyanine dyes Cy2/Cy3/Cy5 (Amersham Biosciences, Little Chalfont, U.K.) prior to electrophoresis. Cyanine dyes (1 mM in DMF) were diluted 1:5 with fresh DMF. Approximately 50 μg of each protein extract (in 4 μL) was mixed with 1 μL of Cy2, Cy3, or Cy5 (0.2 mM), vortexed, and incubated on ice for 30 min in the dark as previously described (*10*). The reactions were quenched by addition of 1 μL of 10 mM lysine, vortexed, and incubated on ice for 10 min in the dark. An equal volume of rehydration buffer [30 mM Tris (pH 8) containing 7 M urea, 2 M thiourea, 4% (w/v) CHAPS, 2% DTT, and 1% (v/v), pH 4−7, IPG buffer] was added so that the final concentrations of DTT and IPG buffer were 1 and 0.5%, respectively. The samples were vortexed and incubated on ice for a further 15 min in the dark. The Cy2-labeled pooled extracts were combined with the Cy3-labeled vehicle extracts and Cy5-labeled compound A (250 mg/kg/day) extracts. A reciprocal mixture was also used to account for any preferential labeling of the CyDyes, such that Cy2-labeled standard pool extracts were combined with Cy5-labeled vehicle extracts and Cy3-labeled compound A extracts (see Table 2). The volume of the combined labeled samples was adjusted to 400 μL with standard rehydration buffer [30 mM Tris (pH 8), 7 M urea, 2 M thiourea, 4% (w/v) CHAPS, 1% DTT, and 0.5% (v/v), pH 4−7, IPG buffer].

Two-Dimensional Gel Electrophoresis. The mixed CyDye-labeled protein solutions were used to rehydrate 18 cm IPG strips (pH 4−7; Amersham Biosciences) for 4 h with no voltage and then for a further 7 h at 30 V. Isoelectric focusing (IEF) was carried out using a step gradient at 500 V for 1 h, 1000 V for 1 h, and 8000 V for 6 h in an IPGphor IEF unit (Amersham Biosciences). The IPG strips were equilibrated for 10 min in 125 mM Tris (pH 6.8) containing 6 M urea, 30% glycerol, 2% SDS, and 65 mM DTT and then for a further 10 min of incubation in the same buffer except that DTT was replaced with 260 mM iodoacetamide. The IPG strips were then sealed with 0.5% agarose in SDS running buffer at the top of slab gels (180 mm × 160 mm × 1 mm) polymerized from 12% (w/v) acrylamide and 0.1% N,N′-methylene bis-acrylamide. The gels were poured between low fluorescent Pyrex glass plates to minimize background fluorescence during scanning. The second-dimension electrophoresis was performed at 20 °C in SE600 tanks (Amersham Biosciences) overnight at 55 V until the bromophenol blue dye front had just run off the base of the gel.

Protein Visualization and Image Analysis. Cy2-, Cy3-, and Cy5-labeled protein images were produced by scanning gels directly between the glass plates using filters specific for each dye's excitation and emission wavelength with the 2920 2D-Master Imager (Amersham Biosciences). The excitation wavelengths were as follows: Cy2, 480 ± 35 nm; Cy3, 540 ± 25 nm; and Cy5, 620 ± 30 nm. The emission wavelengths were 530 ± 30, 590 ± 35, and 680 ± 30 nm, respectively. The images were exported in the form of 16-bit tagged image file format (TIFF) files for analysis. The TIFF images were analyzed automatically using the DeCyder Batch Processor and Differential in-gel Analysis (DIA) software modules (Amersham Biosciences). On individual gels, Cy2-labeled images (from the pooled standard) were compared with either the Cy3 (Cy2:Cy3) or the Cy5 (Cy2:Cy5) images from the individual vehicle and compound A samples using the DIA software. Images from separate gels were compared using the Biological Variation Analysis (BVA) module of the DeCyder software to match gels using the Cy2-labeled pooled standard on each gel to normalize the images. Results were given as standard abundance ratios for each protein spot from the compound A-treated rats relative to the vehicle-treated controls. The statistical significance of each expression level was calculated using Student's *t*-test on the logged ratios (log compound A/vehicle). This analysis is equivalent to doing a paired *t*-test and has increased power by taking into account the pairing of samples within gels. Protein spot expression levels, which showed a statistically significant ($p < 0.05$) increase or decrease on every gel used in the study, were accepted as being differentially expressed between the extracts under comparison.

Protein Identification by Mass Spectrometry. Separate preparative gels electrophoresed with 80 μg of individual vehicle and compound A liver extracts were fixed with 30% methanol and 10% acetic acid for 30 min and then stained with Sypro Ruby (Molecular Probes, Inc., Eugene, OR) overnight. Gels were destained with a 10% methanol and 4% acetic acid solution for

1 h. The resulting fluorescent images were matched to CyDye images using the Melanie III software (GeneProt, Geneva, Switzerland), and protein spots of interest were excised using the ProPic spot picking robot (Genomic Solutions, Huntingdon, Cambs., U.K.). Excised gel spots were digested in situ with sequencing grade porcine trypsin essentially as described by Wilm and co-workers (*11*) using the ProGest digest robot (Genomic Solutions). Aliquots (0.5 μL) of extracted digests were mixed with 0.5 μL of α-cyano-4-hydroxycinnamic acid (10 mg/mL) on matrix-assisted laser desorption ionization time-of-flight (MALDI-TOF) target plate, and peptide mass determinations were carried out using a Voyager-DE STR Biospectrometry Workstation (PE Biosystems, Framingham, MA). Internal mass calibration was achieved using porcine trypsin autolysis digestion products. Proteins were identified by searching the Swiss-Prot and GenPept databases using MS-Fit (Protein Prospector, UCSF, CA). All searches were carried out using a mass window of 10 000−150 000 Da and included rodent and human sequences. The search parameters allowed for carboxyamidomethylation of cysteine, oxidation of methionine, and modification of glutamine to pyroglutamic acid. Positive identifications were accepted with at least six matching peptide masses and at least 30% peptide coverage of the theoretical sequences.

For those spots where MALDI-TOF peptide mapping did not give a protein identification, a Micromass Q-TOF mass spectrometer (Micromass, Manchester, U.K.) with a nanospray source was used for partial sequencing of the peptide mixture (*12*). Five microliters of a proteolytically digested protein solution were loaded into a gold-plated Micromass borosilicate NanoESI probe. This was mounted on the nanoflow source of the mass spectrometer. A potential of 900 V was applied to the emitter, and spectra were acquired. Peptides were observed as either singly, doubly, or triply charged species in the mass-to-charge range of 400−2000. Tandem mass spectrometry with collision-induced dissociation was then performed on selected doubly charged ions to obtain sequence data. The data were processed using MassLynx v 3.4 software and saved as a Sequest file. The parameters used for searching were raw Sequest file, charge state of the precursor ion, taxonomy "*Rattus norvegicus*", enzyme used for digestion (trypsin), one allowed miss cleavage, cysteines modified with iodoacetamide as fixed modification, and oxidized methionines as variable modification. The product ion mass spectra from the nanoES Q-ToF MS/MS analysis were used in Mascot (Matrix Science Inc, Tanuja Chaudhary, U.S.A.) searches of the NCBInr database.

Results

In Vivo Studies. Female rats were dosed once per day for 5 days with either 250 mg/kg/day compound A, 500 mg/kg/day compound A, or vehicle. Treatment-related mortality was observed for three rats (on days 2, 3, and 4) receiving the 500 mg/kg/day dosage. Accumulation of blood in urine, decreased activity, labored breathing, and lateral recumbency were observed for all animals treated with 500 mg/kg/day compound A, whereas no effects were observed among rats receiving the lower 250 mg/kg/day dosage. Decreases in plasma glucose levels and increased ALT and AST activities were observed in both the 250 and the 500 mg/kg/day treatment groups (Table 2). Within the 500 mg/kg/day treatment group, these changes were observed after the second dose and persisted to completion of the study. Whereas within the 250 mg/kg/day treatment group, the changes were observed after the third dose through to the end of the study.

Histology. Histological examination was also carried out to establish any changes linked to toxicity of the compound A. All animals treated with compound A at either the 250 or the 500 mg/kg dosages had pale livers. Histologically, the pale livers correlated with the microscopic finding of hepatocellular vacuolation. The vacuolation (microvesicles) was consistent with lipid-filled vesicles (demonstrated by the Oil Red O staining) and was present in the periportal areas of the livers of the animals in both treatment groups at the earlier time points of the study (Figure 1). During the course of the study, the vacuolation became more diffuse throughout the liver extending to the centrilobular areas and the severity of the vacuolation increased from slight to moderate (data not shown).

Table 1. Experimental Design for 2D DIGE Comparison of Liver Proteomes from Vehicle- and Compound A-Treated Rats[a]

gel no.	Cy2	Cy3	Cy5
1	pooled std.	vehicle 1	compound A 1
2	pooled std.	vehicle 2	compound A 2
3	pooled std.	vehicle 3	compound A 3
4	pooled std.	compound A 1	vehicle 1
5	pooled std.	compound A 2	vehicle 2
6	pooled std.	compound A 3	vehicle 3

[a] Approximately 50 μg of each extract and the pooled standard were labeled with 0.2 nM indicated CyDye, mixed together and electrophoresed on 2D gels as indicated. Liver aliquots from rats treated with 250 mg/kg/day of the compound A compound are indicated compound A.

Table 2. Treatment-Related Serum Biochemical Changes Induced by Compound A[a]

biochemical marker	day of sacrifice	vehicle control	compound A (mg/kg/day) 250	compound A (mg/kg/day) 500
glucose (mg/dL)	1	110	96	104
	2	101	103	40*
	3	110	64*	47*
	4	207	136*	63*
	5	122	101*	48*
AST (U/L)	1	68	74	90
	2	69	89	165*
	3	72	205*	225*
	4	63	94*	207*
	5	66	198*	228*
ALT (U/L)	1	27	30	35
	2	25	34	74*
	3	22	86*	155*
	4	23	41*	127*
	5	25	117*	128*

[a] Animals were sacrificed on the indicated days, 6 h after dosing. *Statistically significant changes.

Proteomics. To identify potential early markers of compound A toxicity, comparative proteomic profiling was carried out on liver tissues obtained from the 250 mg/kg and vehicle treatment groups after the earliest dosing period (day 1, 6 h postdosing) (Table 1). The tissues were extracted sequentially into two fractions containing proteins of differential solubility (*13*). The first fraction contained proteins soluble in 30 mM Tris (pH 8) containing 8 M urea, and the second fraction contained proteins soluble in 30 mM Tris (pH 8) containing 7 M urea, 2 M thiourea, and 4% CHAPS.

The 2D DIGE image obtained from the first protein fraction (Tris−urea) is shown in Figure 2 over the pH 4−7 range IPG strips used. Approximately 800 protein spots were detected by the 2D Master Imager. Five of these spots showed a change in abundance following treatment with compound A as compared with vehicle alone (Table 3). Two of these spots were down-regulated, and three were up-regulated. One of the up-regulated spots was identified by MALDI-TOF mass spectrometry

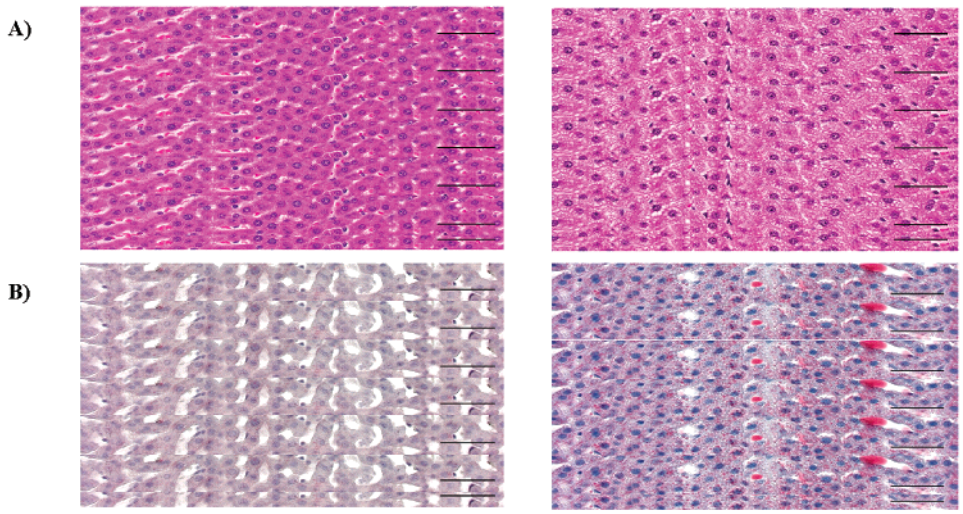

Figure 1. Light microscopic examination of rat liver sections (50 μm) following treatment with 250 mg/kg/day of compound A. (A) Hematoxylin/eosin staining showing the presence of small vacuoles in the cytoplasm of hepatocytes. (B) Oil Red O staining showing small lipid-filled (red staining) vesicles present in the cytoplasm of hepatocytes. Equivalent images were obtained with each of the three livers examined (incidence 3/3 animals).

Table 3. Differentially Expressed Protein Spots in Tris/Urea Protein Extract of Rat Liver Tissue Following Treatment with Compound A[a]

master no.	*T*-test	average ratio	protein ID	accession no.
432[+]	0.037	1.28	AdoMet-Syn	O80483
145[+]	0.027	−1.21	GRP78	P20029
744*	0.01	1.11	pyruvate dehydrogenase	P49432
360*	0.039	1.28	phenylalanine hydroxylase	6981330
936	0.0023	−1.30	ND	ND
521	0.048	1.30	ND	ND
437	0.038	−1.84	ND	ND

[a] The mean compound A:vehicle ratios and levels of significance are given for $n = 3$ separate animal comparisons (each comparison done in duplicate incorporating reciprocal labeling). Only protein spots that were present on every gel and demonstrating changes of ±0.10 with significance $p < 0.05$ were accepted as being differentially expressed. [+]Proteins were identified by MALDI-TOF MS. *Proteins were identified by Q-TOF MS. ND = not determined.

as S-adenosylmethionine synthetase (AdoMet-Syn). This enzyme is involved in the methylation cycle catalyzing the conversion of methionine into homocysteine via S-adenosyl-L-methionine (AdoMet) (*14*). One of the down-regulated proteins was identified as the 78 kDa glucose-regulated protein precursor (GRP78). This protein is thought to be involved in the assembly of multimeric complexes in the lumen of the endoplasmic reticulum (*15*). The other three proteins were not abundant enough to be identified using the pH 4−7 IPG strips. Therefore, the Tris−urea fraction was analyzed using a pH 5−6 IPG strip with a 2-fold higher protein loading (Figure 3). This allowed the identification of two additional up-regulated proteins, which were not detected on the pH 4−7 strip. These were identified as pyruvate dehydrogenase and phenylalanine hydroxylase. Pyruvate dehydrogenase is responsible for the oxidation of pyruvate to acetyl-CoA (*16*), and phenylalanine hydroxylase is involved in the metabolism of phenylalanine to tyrosine by incorporation of one oxygen atom from molecular oxygen and reduction of the other oxygen atom to water (*17*). Two more differentially expressed proteins could not be identified.

The 2D DIGE image from the second fraction (Tris/urea/thiourea/CHAPS) revealed approximately 700 protein spots on pH 4−7 IPG strips (Figure 4). Nineteen of these were differentially expressed following compound A treatment. Thirteen of these were down-regulated, and six were up-regulated (Figure 4). Ten of these 19 proteins were identified either by MALDI-TOF or Q-TOF mass spectrometry. One of the up-regulated spots was identified as the heat shock protein 60 (HSP60), which is a stress responsive protein involved in mitochondrial import and macromolecular assembly (*18*). Another up-regulated protein was identified as the apolipoprotein E precursor (ApoE), which mediates binding, internalization, and catabolism of lipoprotein particles (*19*). Another up-regulated spot was identified as ornithine aminotransferase (OAT). This enzyme is involved in the synthesis of proline (*20*). One of the down-regulated spots was identified as sulfite oxidase (SO), an important enzyme involved in the oxidative degradation of sulfur-containing amino acids (*21*). Four of the down-regulated spots were identified as serum albumin precursors, which appeared as a string of abundant spots on the gels. The remaining down-regulated proteins were identified as peroxiredoxin 4 (PRx IV) and serum paraoxonase (PON), which are involved in protecting cells from oxidative stress (Table 4).

To identify proteins at low abundance from the second fraction, 2D electrophoresis was again carried out using pH 5−6 IPG strips. Two of these proteins were identified by Q-TOF mass spectrometer as 2-oxoisovalerate dehydrogenase β-subunit and acyl-CoA dehydrogenase long chain fatty acid. The 2-oxoisovalerate dehydrogenase is part of the branched chain α-keto acid dehydrogenase and is involved in the metabolism of 2-oxo acids derived from the branched chain amino acids (*22*). Acyl-CoA dehydrogenase is a mitochondrial enzyme that catalyzes the initial step in long fatty acid β-oxidation (*23*).

Discussion

Histological studies showed that compound A caused hepatocellular vacuolation, hypertrophy, inflammation, and cell necrosis following a 15 day dosing regime in monkeys, rats, and mice (data not published). In the current 5 day dosing study, compound A caused hepatocellular vacuolation (steatosis) in rats. To gain some

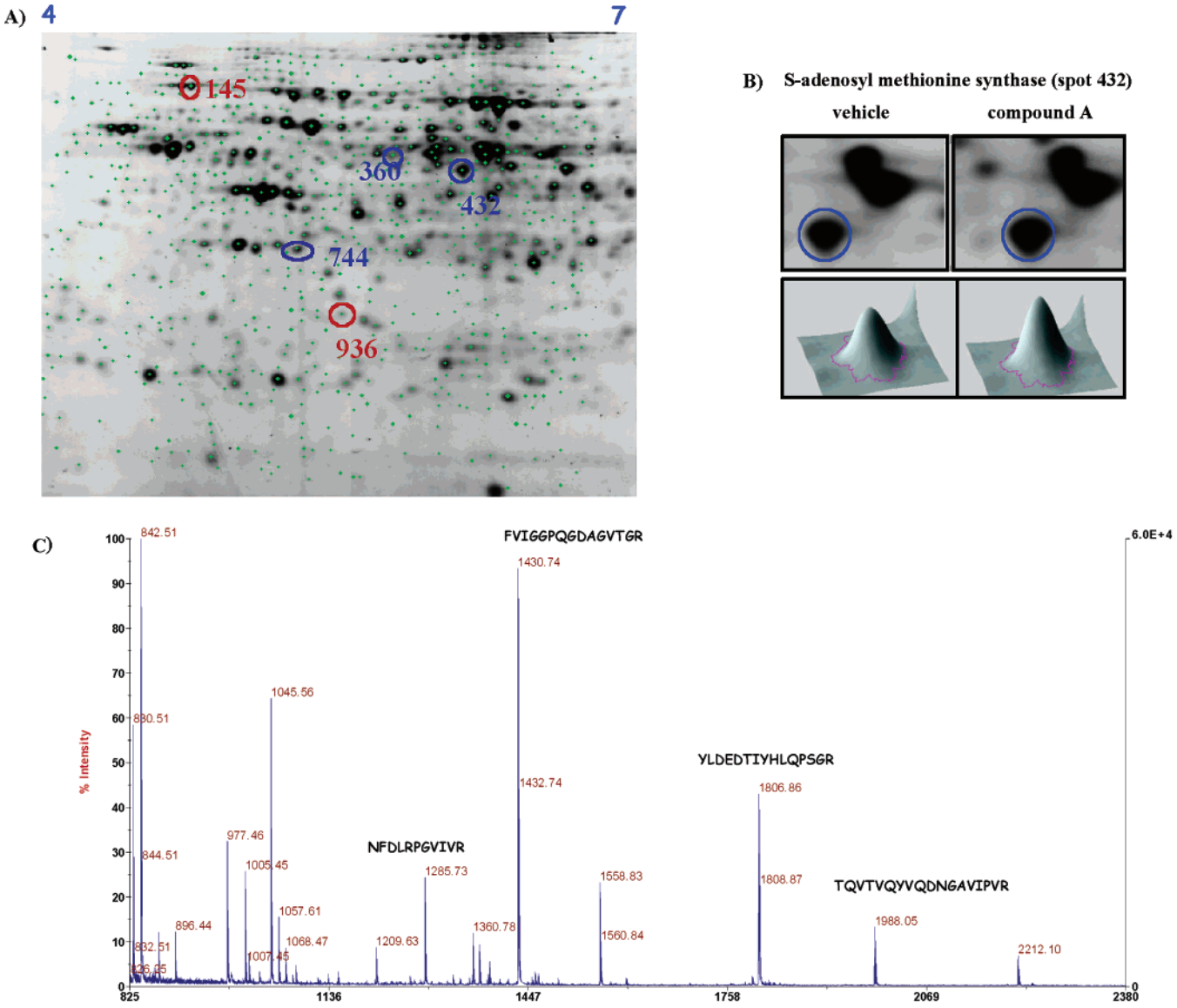

Figure 2. Fluorescent 2D DIGE image showing protein expression differences in Tris/urea protein extract of rat liver tissue following treatment with compound A; pH 4−7 2D gels. (A) Liver protein lysates were labeled with either Cy3 (vehicle) or Cy5 (compound A) and subjected to 2D gel electrophoresis with a Cy2-labeled pooled standard using pH 4−7 IPG strips. Differential expression of proteins between the Cy3 and the Cy5 images was determined as detailed in the Materials and Methods section. Approximate isoelectric points (pI) are shown along the horizontal axis. Blue annotations indicate protein spots which were up-regulated and red annotations indicate protein spots which were down-regulated in compound A-treated rats compared to vehicle-treated controls. The images are representative of similar results obtained from 3 different compound A: vehicle comparisons. The spot numbers are taken from the Master gel image. (B) Enlargement sections of Cy3 (vehicle) and Cy5 (compound A) 2-D images are shown with the selected matched spots highlighted (top panels). The corresponding 3-D images are shown for each selected spot (bottom panels). (C) MALDI-TOF MS spectrum of AdoMet-Syn obtained using a Voyager-DE STR following trypsin digestion of the excised 2-D gel spot as described on the methods section. Four of the key abundant peptides are shown.

insight into the mechanism of compound A toxicity, we have carried out a proteomic analysis of livers from the lowest dose (250 mg/kg/day) and the earliest time point (6 h postdose). This time point was chosen as the livers showed no changes in traditional biochemical markers, despite the histological findings of hepatocellular vacuolation. Thus, any changes in the protein signature might represent early markers of the toxicity. Two-dimensional electrophoresis analysis showed that 26 proteins were changed in rat liver after 6 h of treatment with compound A and 19 of these were identified by mass spectrometry. Some of the protein changes could be ascribed to the cellular pathways associated within the current and previous in vivo histological findings for compound A (*3*). However, markers that could not be linked directly to these phenomena might therefore be involved in other cellular pathways. Further work will be required to understand these protein changes for association with known protein networks.

Previous studies have suggested that drug-induced liver steatosis could result from perturbation of the *β*-oxidation pathway (*5*−*8*). This is important because three of the proteins up-regulated by compound A treatment were pyruvate dehydrogenase, phenylalanine hydroxylase, and 2-oxoisovalerate dehydrogenase, which are involved in metabolic pathways that lead to acetyl-CoA production (*16*, *17*, *22*). Therefore, the up-regulation of these three proteins may be the result of the activation of compensatory mechanisms to overcome the blocked *β*-oxidation of fatty acids to acetyl-CoA. Long chain acyl-

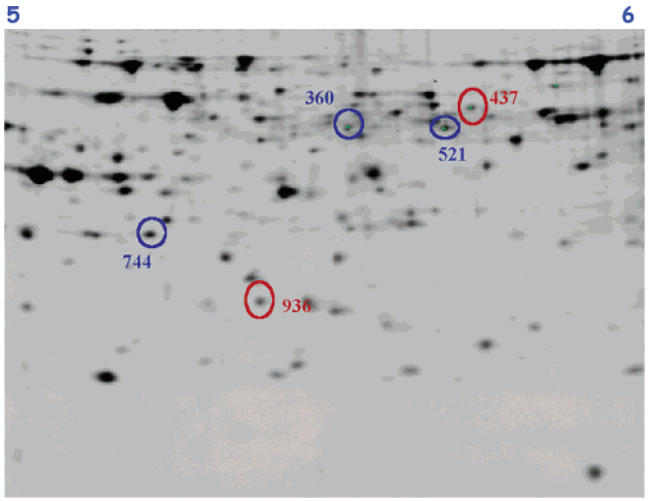

Figure 3. Fluorescent 2D DIGE image showing protein expression differences in Tris/urea protein extract of rat liver tissue following treatment with compound A. pH 5−6 2D gels. Liver protein lysates were labeled with either Cy3 (vehicle) or Cy5 (compound A) and subjected to 2D gel electrophoresis with a Cy2 labeled pooled standard using pH 5−6 IPG strips. Differential expression of proteins between the Cy3 and Cy5 images was determined as detailed in the methods section. Approximate isoelectric points (pI) are shown along the horizontal axis. Blue annotations indicate protein spots that were up-regulated, and red annotations indicate protein spots that were down-regulated in compound A-treated rats as compared to vehicle-treated controls. The images are representative of similar results obtained from three different compound A:vehicle comparisons. The spot numbers are taken from the Master gel image.

Table 4. Differentially Expressed Protein Spots in Tris/Urea/Thiourea/CHAPS Protein Extract of Rat Liver Tissue Following Treatment with Compound A[a]

master no.	*T*-test	average ratio	protein ID	accession no.
577+	0.0084	1.25	HSP60	O80483
1066+	0.0270	1.48	ApoE	P20029
769+	0.0047	1.49	OAT	P29758
455+	0.0016	−1.26	serum albumin precursor	P07724
464+	0.0030	−1.31	serum albumin precursor	P07724
472+	0.0120	−1.30	serum albumin precursor	P07724
473+	0.0037	−1.30	serum albumin precursor	P07724
590+	0.0041	−1.44	SO	Q8R086
852*	0.0015	−1.47	PON	P55159
1230*	0.00064	−1.47	PRx IV	AJ132352
970*	0.0040	1.21	2-oxoisovalerate dehydrogenase	P21839
796*	0.010	1.20	acyl-CoA dehydrogenase long chain	AF049236

[a] The mean compound A:vehicle ratios and levels of significance are given for $n = 3$ separate animal comparisons (each comparison done in duplicate incorporating reciprocal labeling). Only protein spots that were present on every gel and demonstrating changes of ±0.10 with significance $p < 0.05$ were accepted as being differentially expressed. +Proteins were identified by MALDI-TOF MS. *Proteins were identified by Q-TOF MS. ND = not determined.

CoA dehydrogenase (*23*) was also found to be up-regulated, which could result from the accumulation of fatty acid induced by blocked *β*-oxidation as recently described (*3*).

SO was decreased in rat livers within 6 h of compound A treatment. This enzyme catalyzes the oxidation of toxic sulfite (*24*) during degradation of the sulfur-containing amino acids cysteine and methionine. Therefore, a decrease in SO levels might result in accumulation of sulfite. Previous studies have suggested that elevated sulfite could lead to increased triacylglyceride (TG) levels in rat liver (*25*). This is consistent with TG accumulation in liver vacuoles observed in the current study. Another possible outcome of the down-regulation of SO is increased levels of the sulfur-containing amino acid methionine. This could explain the observed up-regulation of AdoMet-Syn in rat livers. AdoMet-Syn is known to be involved in the methylation cycle by catalyzing conversion of methionine to homocysteine via AdoMet, which acts as a methyl group donator for a variety of substrates (*14*). These increased levels of AdoMet-Syn correlate with the increased levels of 1-methyl-nicotinamide found in recent metabonomics work (*3*). A previous report showed that Chinese hamster ovary cells with higher AdoMet-Syn activity have increased sensitivity to oxidative injury due to depletion of ATP and NAD (*26*). The increase in AdoMet levels observed in the present study could be an early marker of toxicity preceding cell death.

Another protein up-regulated by compound A treatment was OAT, a mitochondrial matrix enzyme involved in the synthesis of proline and glutamate (*20*). The increase in OAT is probably a metabolic adaptation to meet increased demands for proline, which is required for the synthesis of collagen and extracellular matrix proteins. This is interesting since we have found liver hypertrophy following 15 day dosing safety studies of both monkeys and mice with compound A at 100 and 200 mg/kg/day (data not shown), and previous studies have demonstrated increased OAT levels in hypertrophied kidney (*27*). Therefore, the significant increase in liver weight following compound A treatment suggests that the increase in OAT might be an early indication of a toxic pathway leading to hypertrophy.

The secretory proteins PON1, serum albumin, and PRx IV were all down-regulated by compound A treatment (*28*). Previous studies have shown that PON1 was significantly decreased in rats treated with carbon tetrachloride (*29*) and albumin was decreased by gadobenate dimeglumine and 2,3,5,6-tetramethyl-*p*-phenyl enediamine, which are all known to cause liver steatosis (*30*, *31*). This suggests that the compound A-induced liver steatosis may be associated with disruption of the secretory pathway. This could be linked to the observed decrease in expression of GRP78. GRP78 is an abundant endoplasmic reticulum luminal protein of the 70 kDa chaperone family and is essential for the correct folding, assembly, and glycosylation of newly synthesized proteins (*15*). Changes in the levels of this protein could have significant physiological consequences due to impaired production of secretory proteins (*32*, *33*) and may therefore explain the reduced expression of PON1, albumin, and PRx IV.

Previous studies have shown that dietary restriction of mice negatively regulates hepatic GRP78 expression at the posttranscriptional level leading to reduced protein expression (*34*). Down-regulation of GRP78 after 6 h of dosing with compound A is not likely to be due to reduction in blood glucose levels. Decreased glucose levels were not observed until after 3 days of dosing with compound A.

In summary, the current proteomics study has identified a signature that correlates with the in vivo findings and highlights potential new pathways associated with the mechanism of toxicity for compound A. The finding that some of the protein changes occurred before the

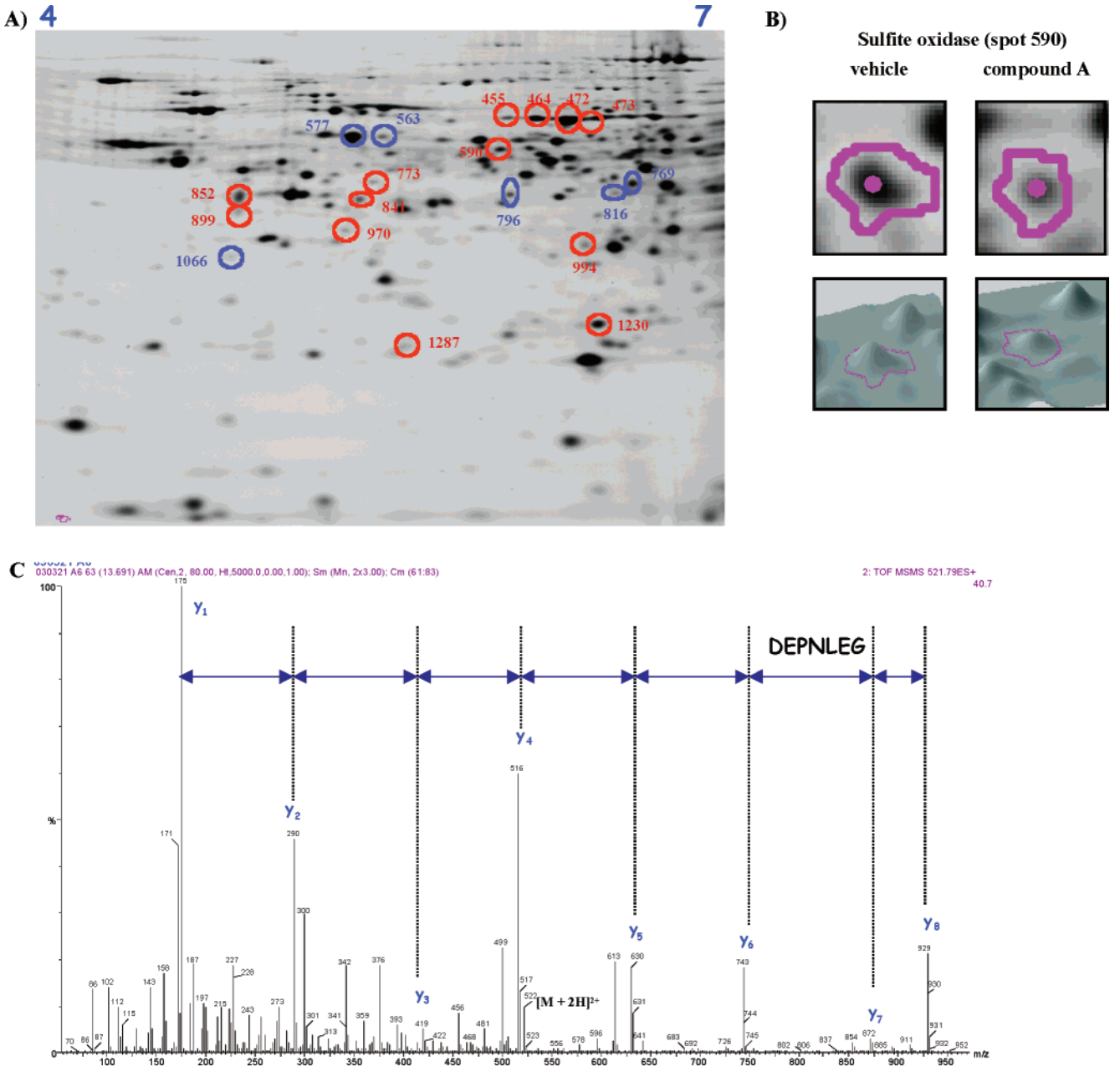

Figure 4. Fluorescent 2D DIGE image showing protein expression differences in Tris/urea/thiourea/CHAPS protein extract of rat liver tissue following treatment with compound A; pH 4−7 2D gels. (A) Liver protein lysates were labeled with either Cy3 (vehicle) or Cy5 (compound A) and subjected to 2D gel electrophoresis with a Cy2-labeled pooled standard using pH 4−7 IPG strips. Differential expression of proteins between the Cy3 and the Cy5 images was determined as detailed in the Materials and Methods section. Approximate isoelectric points (pI) are shown along the horizontal axis. Blue annotations indicate protein spots that were up-regulated, and red annotations indicate protein spots that were down-regulated in compound A-treated rats as compared to vehicle-treated controls. The images are representative of similar results obtained from three different compound A:vehicle comparisons. The spots numbers are taken from the Master gel image. (B) Enlargement of sections of Cy3 (vehicle) and Cy5 (compound A) 2D images with the selected matched spots highlighted (top panels). The corresponding 3D images are shown for each selected spot (bottom panels). (C) Electrospray Q-ToF product ion mass spectrum of [M + 2H] at *m/z* 522 of sulfite oxidase following digestion with trypsin as described in the Materials and Methods section.

onset of clinical biochemistry parameter changes suggests that these could represent potential early markers of toxicity. Further work will be required to establish whether these proteins could be used as a predictive signature for liver steatosis including the use of controls such as known liver inducers of steatosis and time−course experiments. This study suggests that the most productive future studies in toxicology will involve a multifaceted approach including genomics/proteomics (and potentially metabolite profiling/metabonomics) in addition to the determination of conventional clinical biochemistry and pathology parameters. The ultimate goal of proteomics in drug discovery would be to identify markers that are dose-related and can be correlated with the initiation of efficacy or the severity of toxicity. These future potential markers could then be tested using a higher throughput approach than proteomics. A long term aim of proteomics would be to identify the emergence of a signature at an early time point in a readily accessible body fluid, such as serum. Such signatures

could then be used as surrogate markers to help predict the response of individuals and allow tailoring of the therapy to achieve optimal efficacy without side effects.

Acknowledgment. We are grateful to Stan Spence and Anna Chris Hurber for coordinating the link between West Point and Terlings Park sites to make possible this work.

References

(1) Cockerell, G. L., McKim, J. M., and Vonderfecht, S. L. (2002) Strategic importance of research support through pathology. *Toxicol. Pathol. 30* (1), 4−7.

(2) Wilkins, M. R., Williams, K. L., Appel, R. D., and Hochstrasser, D. F. (1997) *Proteome Research: New Frontiers in Functional Genomics*, Springer-Verlag, New York.

(3) Mortishire-Smith, R. J., Skiles, G. L., Lawrence, J. W., Spence, S., Nicholls, A. W., Johnson, B., and Nicholson, J. K. Use of metabonomics to identify impaired fatty acid metabolism as the mechanism of a drug-induced toxicity. *Chem. Res. Toxicol.* Submitted for publication.

(4) Fromenty, B., and Pessayre, D. (1995) Inhibition of mitochondrial beta-oxidation as a mechanism of hepatotoxicity. *Pharmacol. Ther. 67* (1), 101−154.

(5) Berson, A., De Beco, V., Letteron, P., Robin, M. A., Moreau, C., El Kahwaji, J., Verthier, N., Feldmann, G., Fromentry, B., and Pessayre, D. (1998) Steatohepatitis-inducing drugs cause mitochondrial dysfunction and lipid peroxidation in rat hepatocytes. *Gastroenterology 114* (4), 764−774.

(6) Pessayre, D., Bichara, M., Degott, C., Potet, F., Benhamou, J. P., and Feldmann, G. (1979) Perhexiline maleate-induced cirrhosis. *Gastroenterology 76* (1), 170−177.

(7) Simon, J. B., Manley, P. N., Brien, J. F., and Armstrong, P. W. (1984) Amiodarone hepatotoxicity simulating alcoholic liver disease. *N. Engl. J. Med. 311* (3), 167−172.

(8) Zimmerman, H. J. (1978) *Hepatotoxicity: The Adverse Effects of Drugs and Other Chemicals on the Liver*, Appleton-Century-Crofts, New York.

(9) Narahara, S., Yamashita, Y., Makino, T., Shirohata, K., and Otsuji, S. (1980) Determination of serum transaminase activity by pyruvate oxidizing enzymes. *Rinsho Kensa 24* (8), 965−968.

(10) Skynner, H. A., Rosahl, T. W., Knowles, M. R., Salim, K., Reid, L., Cothliff, R., McAllister, G., and Guest, P. C. (2002) Alterations of stress related proteins in genetically altered mice revealed by two-dimensional differential in-gel electrophoresis analysis. *Proteomics 2* (8), 1018−1025.

(11) Wilm, M., Shevchenko, A., Houthaeve, T., Breit, S., Schweigerer, L., Fotsis, T., and Mann, M. (1996) Femtomole sequencing of proteins from polyacrylamide gels by nano-electrospray mass spectrometry. *Nature* (*London*) *379* (6564), 466−469.

(12) Bryant, D. K., Monte, S., Man, W. J., Kramer, K., Bugelski, P., Neville, W., White, I. R., and Camilleri, P. (2001) Principal component analysis of mass spectra of peptides generated from the tryptic digestion of protein mixtures. *Rapid Commun. Mass Spectrom. 15* (6), 418−427.

(13) Molloy, M. P., Herbert, B. R., Walsh, B. J., Tyler, M. I., Traini, M., Sanchez, J. C., Hochstrasser, D. F., Williams, K. L., and Gooley, A. A. (1998) Extraction of membrane proteins by differential solubilization for separation using two-dimensional gel electrophoresis. *Electrophoresis 19* (5), 837−844.

(14) Cantoni, G. L. (1975) Biological methylation. Selected aspects. *Annu. Rev. Biochem. 44*, 435−451.

(15) Little, E., Ramakrishnan, M., Roy, B., Gazit, G., and Lee, A. S. (1994) The glucose-regulated proteins (GRP78 and GRP94): functions, gene regulation, and applications. *Crit. Rev. Eukaryotic Gene Expression 4* (1), 1−18.

(16) Reed, L. J., Fernandez-Moran, H., Koike, M., and Willms, C. R. (1964) Electron microscopic and biochemical studies of pyruvate dehydrogenase complex of escherichia coli. *Science 145*, 930−932.

(17) Robson, K. J. H., Chandra, T., MacGillivray, R. T. A., and Woo, S. L. C. (1982) Polysome immunoprecipitation of phenylalanine hydroxylase mRNA from rat liver and cloning of its cDNA. *Proc. Natl. Acad. Sci. U.S.A. 79* (15), 4701−4705.

(18) Hartl, F. U. (1996) The role of molecular chaperones Hsp70 and Hsp60 in protein folding. *NATO ASI Ser., Ser. H 97* (Posttranscriptional Control of Gene Expession), 193−206.

(19) Yamada, N., Shimano, H., and Yazaki, Y. (1995) Role of apoE on the surface of hepatocytes in chylomicron remnant catabolism. *Int. Congr. Ser. 1066* (Atherosclerosis X), 179−183.

(20) Dekaney, C., Wu, G., and Jaeger, L. A. (2000) Regulation and function of ornithine aminotransferase in animals. *Trends Comp. Biochem. Physiol. 6*, 175−183.

(21) Hille, R. (1996) The Mononuclear Molybdenum Enzymes. *Chem. Rev. 96* (7), 2757−2816.

(22) Massey, L. K., Sokatch, J. R., and Conrad, R. S. (1976) Branched-chain amino acid catabolism in bacteria. *Bacteriol. Rev. 40* (1), 42−54.

(23) Aoyama, T., Ueno, I., Kamijo, T., and Hashimoto, T. (1994) Rat very-long-chain acyl-CoA dehydrogenase, a novel mitochondrial acyl-CoA dehydrogenase gene product, is a rate-limiting enzyme in long-chain fatty acid b-oxidation system. cDNA and deduced amino acid sequence and distinct specificities of the cDNA-expressed protein. *J. Biol. Chem. 269* (29), 19088−19094.

(24) Waley, S. G. (1959) Acidic peptides of the lens. V. S-Sulfoglutathione. *Biochem. J. 71*, 132−137.

(25) Lovati, M. R., Manzoni, C., Daldossi, M., Spolti, S., and Sirtori, C. R. (1996) Effects of sub-chronic exposure to SO2 on lipid and carbohydrate metabolism in rats. *Arch. Toxicol. 70* (3−4), 164−173.

(26) Sanchez-Gongora, E., Pastorino, J. G., Alvarez, L., Pajares, M. A., Garcia, C., Vina, J. R., Mato, J. M., and Farber, J. L. (1996) Increased sensitivity to oxidative injury in Chinese hamster ovary cells stably transfected with rat liver S-adenosylmethionine synthetase cDNA. *Biochem. J. 319* (3), 767−773.

(27) Natesan, S., and Reddy, S. R. R. (2001) Compensatory changes in enzymes of arginine metabolism during renal hypertrophy in mice. *Comp. Biochem. Physiol., Part B: Biochem. Mol. Biol. 130B* (4), 585−595.

(28) Mackness, M. I., Mackness, B., Durrington, P. N., Connelly, P. W., and Hegele, R. A. (1996) Paraoxonase: biochemistry, genetics and relationship to plasma lipoproteins. *Curr. Opin. Lipidol. 7* (2), 69−76.

(29) Ferre, N., Camps, J., Cabre, M., Paul, A., and Joven, J. (2001) Hepatic paraoxonase activity alterations and free radical production in rats with experimental cirrhosis. *Metab. Clin. Exp. 50* (9), 997−1000.

(30) Draper, R. P., Waterfield, C. J., York, M. J., and Timbrell, J. A. (1994) Studies on the muscle toxicant 2,3,5,6-tetramethyl-*p*-phenylenediamine: effects on various biomarkers including urinary creatine and taurine. *Arch. Toxicol. 69* (2), 111−117.

(31) Katsutani, N., Sagami, F., Tirone, P., Morisetti, A., Bussi, S., and Mandella, R. C. (1999) General toxicity study of gadobenate dimeglumine formulation (E7155). (4). 4-week repeated dose intravenous toxicity study followed by 4-week recovery period in dogs. *J. Toxicol. Sci. 24* (Suppl. 1), 41−60.

(32) Dorner, A. J., Krane, M. G., and Kaufman, R. J. (1988) Reduction of endogenous GRP78 levels improves secretion of a heterologous protein in CHO cells. *Mol. Cell. Biol. 8* (10), 4063−4070.

(33) Dorner, A. J., Wasley, L. C., and Kaufman, R. J. (1992) Overexpression of GRP78 mitigates stress induction of glucose regulated proteins and blocks secretion of selective proteins in Chinese hamster ovary cells. *EMBO J. 11* (4), 1563−1571.

(34) Tillman, J. B., Mote, P. L., Dhahbi, J. M., Walford, R. L., and Spindler, S. R. (1996) Dietary energy restriction in mice negatively regulates hepatic glucose-regulated protein 78 (GRP78) expression at the posttranscriptional level. *J. Nutr. 126* (2), 416−423.

TX034203N